

Reflection-influenced circularly polarised luminescence in dye-embedded polymer-stabilised cholesteric liquid crystal films

Ting Lian, Runwei Yu, Wei Liu,* Yi Li and Yonggang Yang*

State and Local Joint Engineering Laboratory for Novel Functional Polymeric Materials, Jiangsu Key Laboratory of Advanced Functional Polymer Design and Application, Jiangsu Engineering Laboratory of Novel Functional Polymeric Materials, Department of Polymer Science and Engineering, College of Chemistry, Chemical Engineering and Materials Science, Soochow University, Suzhou 215123, China. Email: W. Liu, weiliu@suda.edu.cn; Y. Yang, ygyang@suda.edu.cn.

Table of Contents

Scheme 1 Synthetic route to TPT.

Scheme S2. Schematic illustration of CPL measurements.

Experimental Section

Table S1 Optical data of TPT measured in different solvents.

Table S2 Main calculated optical transitions for TPT.

Table S3 Crystal measurement and refinement data for TPT.

Table S4 Optical data for compound TPT measured in solid-state.

Table S5 and 6 Mass percentages of compounds in the CLC mixtures with and without dye.

Fig. S1 UV-vis absorption and emission spectra of TPT in different solvents.

Fig. S2 Energy level diagram of frontier molecular orbitals, and orbital distributions for TPT.

Fig. S3 UV-vis absorption and excitation spectra for TPT in a DMF-water mixture at $f_w = 90\%$.

Fig. S4 DLS profile for TPT in a DMF-water mixture at $f_w = 90\%$.

Fig. S5 Crystal packing diagram along the *b*-axis.

Fig. S6 UV-vis absorption and excitation spectra of solid powder of TPT before and after grinding.

Fig. S7 CIE 1931 spectral chromaticity coordinates of TPT in different solid states.

Fig. S8 Powder X-ray diffraction and simulated patterns of TPT.

Fig. S9 UV-vis-NIR reflectance of CLC mixtures taken before photopolymerization.

Fig. S10 POM image of LC242 with 1 wt% of TPT and 4.6 wt% of CA at 60 °C.

Fig. S11 Plots of λ_{\max} vs DRCD and DRUV-vis-NIR for TPT-PSCLC films.

Fig. S12 FE-SEM images the TPT-PSCLC films with (a) 4.6 and (b) 6.3 wt% of CA.

Fig. S13 Emission spectra of TPT-PSCLC films ($\lambda_{\text{ex}} = 340$ nm).

Fig. S14 (a) CPL spectra and (b) g_{lum} values of the TPT-PMMA film; (c) CPL spectra and (d) g_{lum} values of circularly polarized light.

Fig. S15 UV-vis-NIR reflectance of PSCLC films without dye TPT.

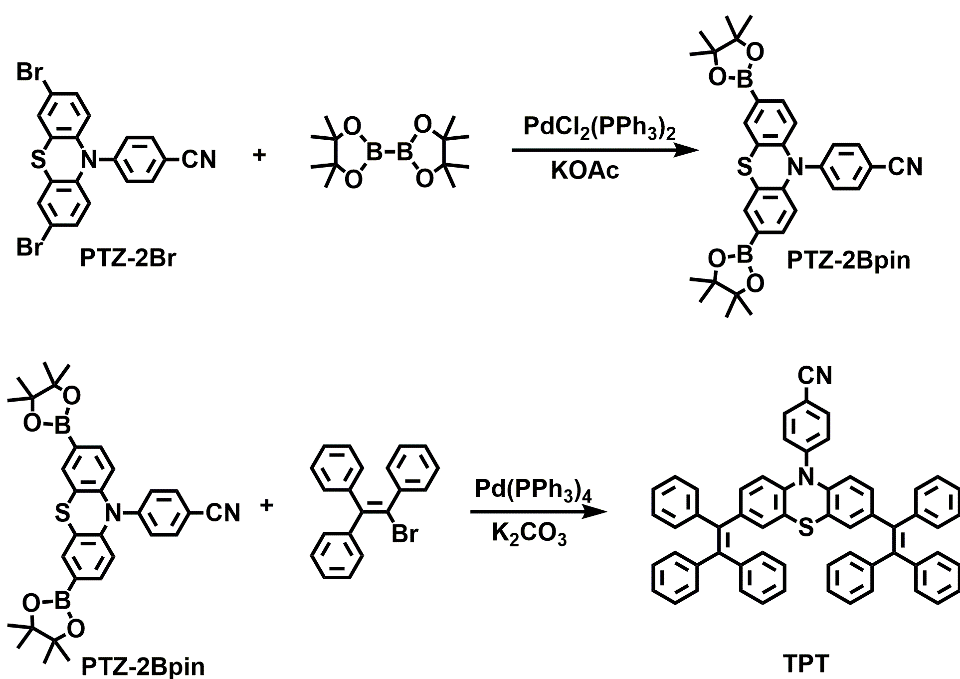
Fig. S16 Cross-sectional FE-SEM images the PSCLC film with 5.6 and 6.3 wt% of CA.

Fig. S17 g_{lum} values of TPT-PMMA film (1.0 wt% of dye) placed in front of PSCLC films.

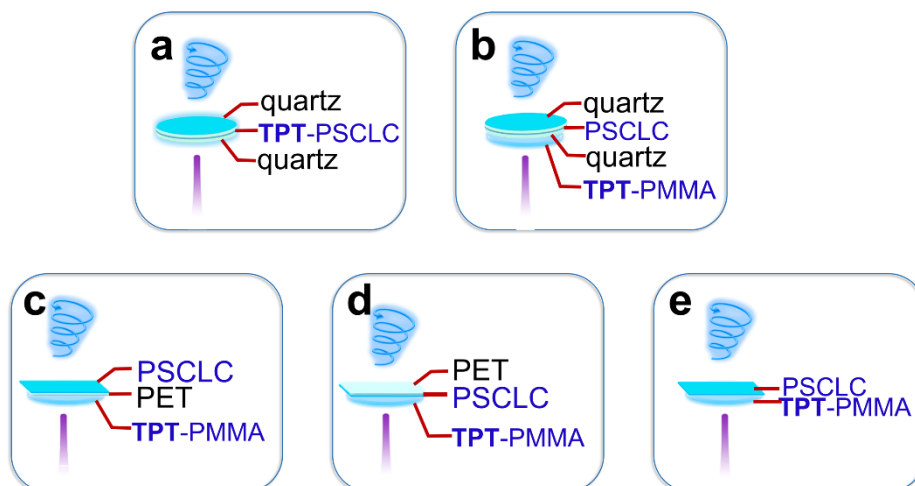
Fig. S18 Cross-sectional FE-SEM images of the PSCLC coated PET films with different thicknesses.

Fig. S19 Transmittance spectra of PSCLC coated PET films (with different thickness) without dye.

Fig. S20 (a) CPL spectra and (b) g_{lum} values of TPT-PMMA film (1.0 wt% of dye) located in front of PSCLC coated PET films with different thicknesses excited by circularly polarized light.



Scheme S1. Synthetic route to TPT.



Scheme S2. Schematic illustration of the CPL characterisations (excited by nonpolarized light).

Experimental Section

General information

Compounds 10*H*-phenothiazine, 4-fluorobenzonitrile, sodium hydride (NaH, 60%), *N*-bromosuccinimide, bis(pinacolato)diboron, $\text{PdCl}_2(\text{PPh}_3)_2$ and KOAc were obtained from Aladdin Chemical Co., Ltd (Shanghai, China). Bromotriphenylethylene, potassium carbonate, and $\text{Pd}(\text{PPh}_3)_4$ were obtained from Energy Chemical Co., Ltd (Shanghai, China). *N,N*-Dimethylformamide

(DMF), petroleum ether (PE), dichloromethane (DCM), ethyl acetate, 1,4-dioxane, and toluene were purchased from Shanghai Lingfeng Chemical Reagent Co., Ltd. Cyclohexanone was purchased from Yonghua Co., Ltd (Jiangsu, China). Polyethylene terephthalate (PET) films were purchased from Nanya plastics Co., Ltd (Nantong, China). ^1H NMR and ^{13}C NMR spectra were recorded on an Vnmrs-300 (Agilent, USA) using tetramethylsilane (TMS) as an internal standard. Mass spectra (MS) were obtained using an UltrafleXtreme MALDI TOF/TOF spectroscope (Bruker, USA). Elemental analysis was measured on an Flashsmart instrument (Thermo Scientific, Germany). FT-IR spectra were performed on a VERTEX 70 spectrometer (Bruker, Germany) at 4.0 cm^{-1} resolution by averaging over 16 scans. Dynamic light scattering (DLS) measurements were performed on a Zetasizer Nano ZS90 (Malvern, USA). Powder X-ray diffraction (PXRD) data were recorded on a Bruker D8 Advance (Germany) X-ray Powder diffractometer with Cu $K\alpha$ radiation ($\lambda = 1.54056\text{ \AA}$). The simulated PXRD patterns were acquired from single crystal structure data using the Mercury 1.4.1 program. The photoisomerization studies were conducted using UV-LED series equipment (UVSF81T, 365 nm, 400 mW cm^{-2} , output power) produced by FUTANSI Electronic Technology Co., Ltd (Shanghai, China). The UV-LED parallel light source is equipped with double aspherical quartz lenses to produce parallel light with a parallel half angle of less than 2° . The photopolymerization were conducted using a high-pressure Hg lamp (MINHIO 4012-20, 350-450 nm, 1000W, input power), produced by MINHIO Intelligent Equipment Co., Ltd (Shenzhen, China). FE-SEM images were obtained using a Hitachi S-4800 operating (Ibaraki prefecture, Japan) at 3.0 kV. To obtain good morphology, cross-sectional SEM samples are prepared in liquid nitrogen. DRCD spectra were measured by using a JASCO 815 spectrometer (Tokyo, Japan). UV-vis-NIR spectra were measured by a UV-vis-NIR spectrophotometer (UV3600, Shimadzu, Japan). The POM images of the target compounds were taken using a Leica Microsystems CMS GmbH fitted with a Linkam LTS420 hot stage. Fluorescence spectra and quantum yields were measured by FLS 980 (Edinburgh Instrument, UK). CPL spectra were measured on JASCO CPL-300 (JASCO, Japan). In the CPL measurements, the excitation wavelength was 340 nm, the scan speed was 500 nm/min, the number of scans

was 1, the slit width was 3000 μm for excitation and the monitor, and the time constant of PMT (D.I.T.) was 1 s. The value of g_{lum} is experimentally defined as $g_{\text{lum}} = \Delta I/I = \Delta I/\text{PL (DC in volts)} = [\text{ellipticity}/(32980/\ln 10)] / \text{PL (DC in volts)}$ at a CPL wavelength, while PL (DC in volts) stands for total luminescence I , and $I = I_L + I_R$.^{S1} To eliminate the effect of line polarization luminescence of the films, a plate holder was used to allow the samples to rotate 360°, and the CPL spectra from 4 scans at 90° intervals in the four directions were algebraically averaged. Since the helical structures in all PSCLC films were perpendicular to the surface, the CPL spectra and g_{lum} values for each side of the thin film were similar. LC242 was given by Soochiral Chemical Sci. & Techn. Co., Ltd (Suzhou, China). Photoinitiator 907 was purchased from Aladdin Chemical Co., Ltd (Shanghai, China). The TPT-PMMA film was deposited onto a polished circular-shape quartz plate (2 cm in diameter, 1 mm in thickness) by spin coating with a spin coater (model KW-4A, Beijing, China). The chiral additive CA was prepared by the method reported by our group.^{S2} The precursor compound 4-(3,7-dibromo-10H-phenothiazine-10-yl)benzotrile (PTZ-2Br) was synthesized according to the literature.^{S3}

Synthesis of 4-(3,7-bis(4,4,5,5-tetramethyl-1,3,2-dioxaborolan-2-yl)-10H-phenothiazin-10-yl)benzotrile (PTZ-2Bpin)

Under an N_2 atmosphere, **PTZ-2Br** (3.0 g, 6.5 mmol), bis(pinacolato)diboron (4.95 g, 19.5 mmol), $\text{PdCl}_2(\text{PPh}_3)_2$ (0.3 g, 0.43 mmol), KOAc (1.90 g, 19.5 mmol) were dissolved in 1,4-dioxane (100 mL) in a 250 mL of Schlenk flask. The reaction mixture was heated to 100 °C, and stirred for 24 h. After cooling to room temperature, diatomite was added and filtered. The filtrate was washed with water and extracted with dichloromethane three times. The organic phases were combined, and dried with anhydrous MgSO_4 . After the removal of the solvent under reduced pressure, a yellow solid was obtained. After being washed with ethyl acetate, a light-yellow powder **PTZ-2Bpin** was obtained (71% yield). FT-IR ν_{max} : 2976, 2230, 1582, 1352, 1304, 1259, 1145, 1101, 963, 886 and 826 cm^{-1} . ^1H NMR (300 MHz, CDCl_3 , TMS) δ : 7.72-7.62 (m, 4H), 7.50 (dd, $J = 8.1$ Hz, 1.4 Hz, 2H), 7.33-7.27 (m, 2H), 6.69 (d, $J = 8.0$ Hz, 2H), 1.33 (s, 24H) ppm. ^{13}C

NMR (101 MHz, CDCl₃) δ : 143.4, 143.2, 142.9, 142.0, 139.3, 133.6, 131.2, 130.7, 130.4, 127.9, 127.8, 127.7, 126.8, 126.7, 123.8, 119.3, 118.4, 104.9 *ppm*. MS (MALDI-TOF) *m/z* C₃₁H₃₅B₂N₂O₄S [M+H]⁺, calculated: 553.243; Found: 553.500. EA: Calcd. for C₃₁H₃₄B₂N₂O₄S, C 67.42, H 6.21, N 5.07%; Found, C 67.45, H 6.13, N 5.27%.

Synthesis of 4-(3,7-bis(1,2,2-triphenylvinyl)-10H-phenothiazin-10-yl)benzonitrile (TPT)

PTZ-2Bpin (2.0 g, 3.6 mmol), bromotriphenylethylene (3.6 g, 10.8 mmol), potassium carbonate (2.5 g, 18 mmol), Pd(PPh₃)₄ (0.25 g, 0.2 mmol) were added to a mixed solvent of 45 mL toluene and 30 mL H₂O. The mixture was stirred at 110 °C under an N₂ atmosphere for 24 h. Then the mixture was poured into water and extracted with DCM three times. The organic phases were combined and dried with anhydrous MgSO₄. After removal of the solvent under reduced pressure, the crude product was purified by column chromatography on silica gel using DCM/PE (v:v = 1:1) as the eluent to afford **TPT** as a light-yellow powder (69% yield). *m.p.* 253.2 °C. FT-IR ν_{\max} : 2223, 1750, 1606, 1590, 1504, 1491, 1470, 1173, 1156, and 1075 cm⁻¹. ¹H NMR (300 MHz, DMSO-*d*₆, TMS) δ : 6.74 (d, *J* = 8.1 Hz, 2H), 6.77-6.88 (m, 4H), 6.90-7.43 (m, 32H), 7.79 (d, *J* = 8.5 Hz, 2H) *ppm*. ¹³C NMR (101 MHz, CDCl₃) δ : 146.9, 144.0, 134.9, 134.4, 134.2, 133.8, 133.7, 127.2, 126.95, 125.7, 123.5, 120.7, 119.6, 118.8, 108.0, 84.0, 83.1, 24.8, 24.6 *ppm*. MS (MALDI-TOF) *m/z* C₅₉H₄₀N₂S [M+H]⁺, calculated: 809.291; Found: 809.920. EA: Calcd. for C₅₉H₄₀N₂S, C 87.59, H 4.98, N 3.46%; Found, C 87.23, H 5.08, N 3.62%.

Preparation of TPT-PSCLC films prepared between two quartz plates.

The **TPT-PSCLC** films were prepared by photopolymerization of the mixture of LC242 doped with 1.0 wt% of **TPT**, and 3.0 wt% of 907 with different amounts of CA (Table S5). These mixtures were dissolved in DCM and 150 μ L of the mixture was taken on a quartz plate. The quartz plate was heated to 80 °C to evaporate the solvent. Then a second quartz plate was placed on top and the mixture was allowed to spread throughout the quartz plate and then slowly cooled to room temperature. Finally,

the material was photopolymerized for 10 s after exposing it to 365 nm UV light with 300 mW/cm².

Preparation of TPT-PMMA film.

The PMMA film with TPT was prepared at 120 °C. An acetone solution of the PMMA/TPT mixture was prepared at the weight ratio of 99/1. A thin film was prepared by spin coating on the surface of a quartz plate. Finally, the TPT-PMMA film was obtained by keeping the coated quartz plate at 120 °C for 5 min.

Preparation of PSCLC films prepared between two quartz plates.

The PSCLC films were prepared by photopolymerization of the mixture of LC242 doped with 3 wt% of 907 with different amounts of CA (Table S6). These mixtures were dissolved in DCM and 150 µL of the mixture was taken on a quartz plate. The quartz plate was heated to 80 °C to evaporate the solvent. Then a second quartz plate was placed on top and the mixture was allowed to spread throughout the quartz plate. After slowly cooling to room temperature, the material was photopolymerized for 10 s after exposing it to a 365 nm UV lamp with 300 mW/cm².

Preparation of PSCLC coatings with different thicknesses on PET

A mixture of LC242/CA/907 was prepared at the weight ratio of 91.4/5.6/3.0, which was dissolved in a solvent mixture of cyclohexanone and ethyl acetate to form a solution with 20 wt% of solid content. The solutions were coated on rubbing-oriented PET film using a Mayer bar for controlling thickness. Coating with 10, 20, and 30 µm Mayer bars to obtain films with different thicknesses. After coating, the samples were heated at 100 °C for 6-10 min to evaporate the solvent. Finally, the films were obtained by curing with a high-pressure Hg lamp (1000 W).

Preparation of the multicolour-patterned PSCLC coating on a PET film.

A mixture of LC242/CA/TPT/907 was prepared at the weight ratio of 89.7/6.3/1.0/3.0, which was dissolved in a solvent mixture of cyclohexanone and ethyl acetate to form a solution with 20 wt% of solid content. The mixtures described above were configured in a solvent mixture of cyclohexanone and ethyl acetate to solutions with 20% solid content. The solutions were coated on rubbing-oriented PET film using a Mayer bar

with 20 μm for controlling thickness. After coating, the samples were heated at 100 $^{\circ}\text{C}$ for 6-10 min to evaporate the solvent. The photoisomerization was carried out through a photomask under UV-LED series equipment (400 mW cm^{-2}) at a distance of 20 cm for 7 s and 14 s. Finally, the colourful painting was obtained by curing with a high-pressure Hg lamp (1000 W).

X-ray crystallography

Suitable single crystals for the X-ray crystallographic analysis of compound **TPT** were obtained by the slow evaporation of $\text{CH}_3\text{CN}/\text{DCM}$ (v/v, 1/1) solutions at room temperature. Crystal determination was performed with a Bruker SMART APEX II CCD diffractometer equipped with graphite-monochromated Mo $K\alpha$ radiation ($\lambda = 0.71073 \text{ \AA}$). The structures were solved by direct methods and refined by full-matrix least squares methods on F^2 using SHELX^{S4} under OLEX2.^{S5} The hydrogen atoms were assigned with common isotropic displacement factors, and included in the final refinement by use of geometrical restraints. CCDC 2237856 contains the supplementary crystallographic data for this paper. These data can be obtained free of charge from the Cambridge Crystallographic Data Centre via www.ccdc.cam.ac.uk/data_request/cif.

Computation details

All calculations were carried out with Gaussian 09 programs.^{S6} The structural optimizations of **TPT** were started from the geometry obtained from single-crystal X-ray diffraction. Density functional theory (DFT) and time-dependent DFT (TDDFT) were carried out at the B3LYP functional level by using 6-31G(d) for all atoms.^{S7-9}

References

- S1 (a) S. Ito, K. Ikeda, S. Nakanishi, Y. Imai and M. Asami, *Chem. Commun.*, 2017, 53, 6323–6326; (b) H. Chen, Z. G. Gu and J. Zhang, *J. Am. Chem. Soc.*, 2022, **144**, 7245–7252
- S2 R. Yu, Y. Cao, K. Chen, Y. Li, W. Liu, B. Li, H. Li and Y. Yang, *ACS Appl. Mater. Interfaces*, 2022, **14**, 38228–38234.
- S3 I. T. Choi, M. J. Ju, S. H. Song, S. G. Kim, D. W. Cho, C. Im and H. K. Kim, *Chem. Eur. J.*, 2013, **19**, 15545–15555.
- S4 G. M. Sheldrick, *Acta Crystallogr. A*, 2008, **64**, 112–122.
- S5 O. V. Dolomanov, L. J. Bourhis, R. J. Gildea, J. A. K. Howard and H. Puschmann, OLEX2: A complete structure solution, refinement and analysis program. *J. Appl. Crystallogr.*, 2009, **42**, 339–341.
- S6 M. J. Frisch, G. W. Trucks, H. B. Schlegel, G. E. Scuseria, M. A. Robb, J. R. Cheeseman,

G. Scalmani, V. Barone, B. Mennucci, G. A. Petersson, H. Nakatsuji, M. Caricato, X. Li, H. P. Hratchian, A. F. Izmaylov, J. Bloino, G. Zheng, J. L. Sonnenberg, M. Hada, M. Ehara, K. Toyota, R. Fukuda, J. Hasegawa, M. Ishida, T. Nakajima, Y. Honda, O. Kitao, H. Nakai, T. Vreven, J. A. J. Montgomery, J. E. Peralta, F. Ogliaro, M. Bearpark, J. J. Heyd, E. Brothers, K. N. Kudin, V. N. Staroverov, R. Kobayashi, J. Normand, K. Raghavachari, A. Rendell, J. C. Burant, S. S. Iyengar, J. Tomasi, M. Cossi, N. Rega, J. M. Millam, M. Klene, J. E. Knox, J. B. Cross, V. Bakken, C. Adamo, J. Jaramillo, R. Gomperts, R. E. Stratmann, O. Yazyev, A. J. Austin, R. Cammi, C. Pomelli, J. W. Ochterski, R. L. Martin, K. Morokuma, V. G. Zakrzewski, G. A. Voth, P. Salvador, J. J. Dannenberg, S. Dapprich, A. D. Daniels, O. Farkas, J. B. Foresman, J. V. Ortiz, J. Cioslowski and D. J. Fox, *Gaussian 09, revision D.01 Gaussian, Inc.: Wallingford, CT*, 2013.

S7 C. Lee, W. Yang and R. G. Parr, *Phys. Rev. B*, 1988, **37**, 785–789.

S8 B. Miehlich, A. Savin, H. Stoll and H. Preuss, *Chem. Phys. Lett.*, 1989, **157**, 200–206.

S9 A. D. Becke, *J. Chem. Phys.*, 1993, **132**, 5648–5652.

Table S1 Optical data of **TPT** measured in different solvents (ca. 10 μ M).

Solvent	$\lambda_{abs}^{max} / \text{nm}^a$	$\lg \epsilon^b$	$\lambda_{em}^{max}(\lambda_{ex}) / \text{nm}$	Stokes shift/ nm
MeOH	290, 391 (sh)	4.7	512 (340)	222
Tol	288, 392 (sh)	4.8	516 (340)	228
THF	290, 390 (sh)	4.7	532 (340)	242
DCM	290, 388 (sh)	4.6	542 (340)	252
DMF	290, 390 (sh)	4.9	550 (340)	260
CH ₃ CN	291, 389 (sh)	4.7	558 (340)	267

^a All of the values correspond to the strongest absorption peaks. ^b Molar absorption coefficients are in the maximum of the highest peak.

Table S2 Main calculated optical transitions for **TPT** at the level of B3LYP/6-31G(d).

Orbital excitation	Composition	f^a	λ^b / nm (calcd.)
HOMO \rightarrow LUMO	0.69694	0.20	379
HOMO-1 \rightarrow LUMO	0.68987	0.33	347
HOMO \rightarrow LUMO+1	0.64555	0.13	342
HOMO-1 \rightarrow LUMO+1	0.60856	0.17	317

^a Oscillator strength; ^b Calculated peaks of UV–vis spectra.

Table S3 Crystal measurement and refinement data for **TPT**.

CCDC Number	2237856
Empirical formula	C ₅₉ H ₄₀ N ₂ S
Formula weight	808.99
Temperature/K	130.0
Crystal system	monoclinic
Space group	P2 ₁ /c
<i>a</i> /Å	31.8064(13)
<i>b</i> /Å	9.4999(4)
<i>c</i> /Å	15.0847(6)
<i>α</i> /°	90
<i>β</i> /°	97.312(2)
<i>γ</i> /°	90
Volume/Å ³	4520.9(3)
Z	4
ρ_{calc} g/cm ³	1.189
μ /mm ⁻¹	0.611
<i>F</i> (000)	1696.0
Crystal size/mm ³	0.01 × 0.005 × 0.005
Radiation	GaK α (λ = 1.34138)
2 θ range for data collection/°	4.874 to 127.14
Index ranges	-42 ≤ <i>h</i> ≤ 42, -12 ≤ <i>k</i> ≤ 12, -20 ≤ <i>l</i> ≤ 20
Reflections collected	132525
Independent reflections	11257 [R _{int} = 0.0703, R _{sigma} = 0.0355]
Data/restraints/parameters	11257/1602/560
Goodness-of-fit on <i>F</i> ²	1.077
Final <i>R</i> indexes [<i>I</i> ≥ 2 σ (<i>I</i>)]	R ₁ = 0.0617, wR ₂ = 0.1934
Final <i>R</i> indexes [all data]	R ₁ = 0.0797, wR ₂ = 0.2081
Largest diff. peak/hole / e Å ⁻³	1.78/-0.30

Table S4 Optical data for compound **TPT** measured in solid-state.

$\lambda_{\text{em}}^{\text{max}}$ / nm	$\Phi_{\text{F}}^{\text{a}}$ %	τ^{b} / ns	k_{r}^{c} (10 ⁹ s ⁻¹)	k_{nr}^{d} (10 ⁹ s ⁻¹)
470	90.6	2.5	0.362	0.037

^a Fluorescence quantum yields (Φ) are measured by the absolute method. ^b Emission lifetime collected at their respective emission maxima. ^c Radiative decay constants $k_{\text{r}} = \Phi_{\text{F}}/\tau$. ^d Non-radiative decay constants $k_{\text{nr}} = (1-\Phi_{\text{F}})/\tau$.

Table S5 Mass percentages of compounds in the **TPT-CLC** mixtures between two

layers of quartz plates.

	Purple	Blue	Green	Yellow	Red	NIR
LC242	89.7	90.1	90.6	91.1	91.4	92.8
CA	6.3	5.9	5.4	4.9	4.6	3.2
TPT	1.0	1.0	1.0	1.0	1.0	1.0
907	3.0	3.0	3.0	3.0	3.0	3.0

Table S6 Mass percentages of compounds in the CLC mixtures (without dye) between two layers of quartz plates.

	Purple	Blue	Sky blue	Green	Yellow	Red	NIR
LC242	90.7	91.1	91.4	91.8	92.4	92.6	93.8
CA	6.3	5.9	5.6	5.2	4.6	4.4	3.2
907	3.0	3.0	3.0	3.0	3.0	3.0	3.0

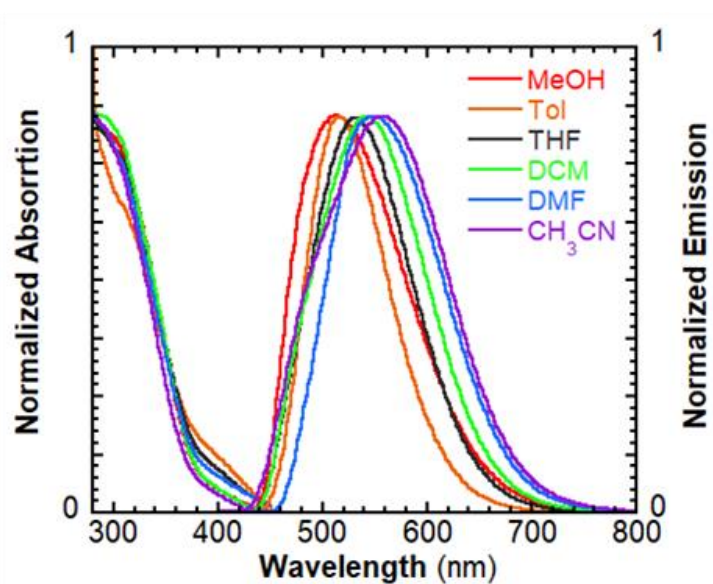


Fig. S1 UV-vis absorption and emission spectra of **TPT** in different solvents (10 μ M).

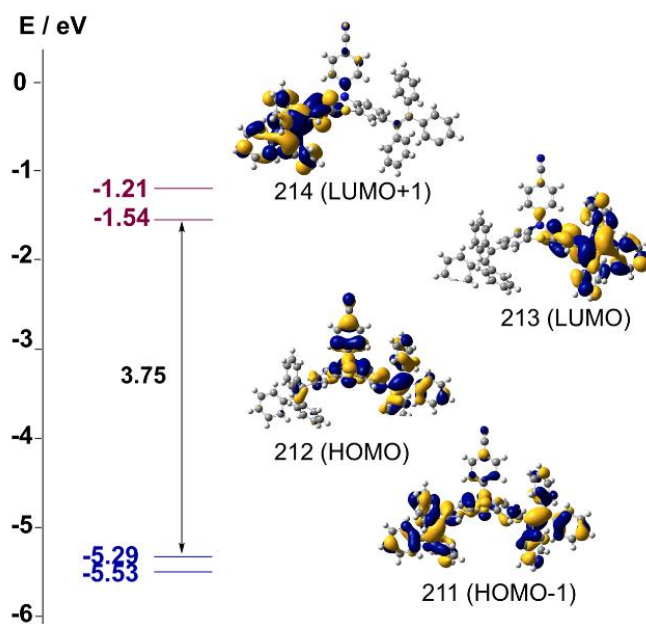


Fig. S2 Energy level diagram of some frontier molecular orbitals, and orbital distributions for **TPT**.

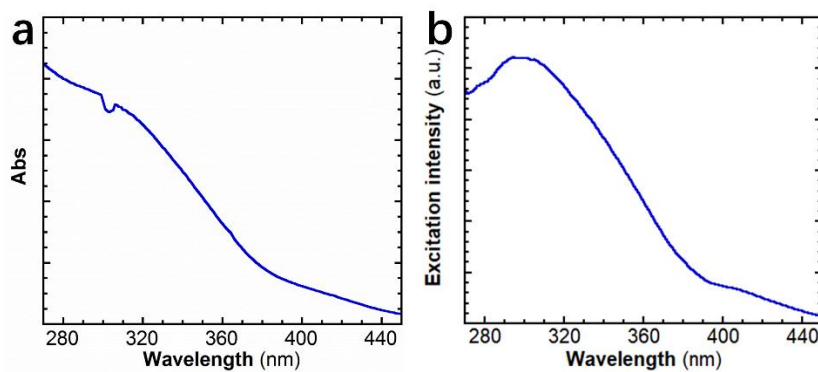


Fig. S3 (a) UV-vis absorption and (b) excitation spectra for **TPT** in a DMF-water mixture at $f_w = 90\%$, at a concentration of $10 \mu\text{M}$.

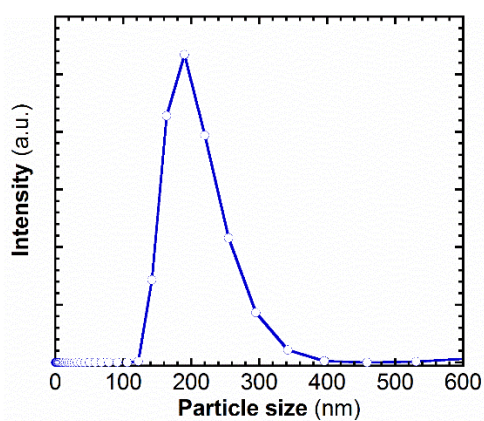


Fig. S4 DLS profile for **TPT** in a DMF-water mixture at $f_w = 90\%$, at a concentration of $10 \mu\text{M}$.

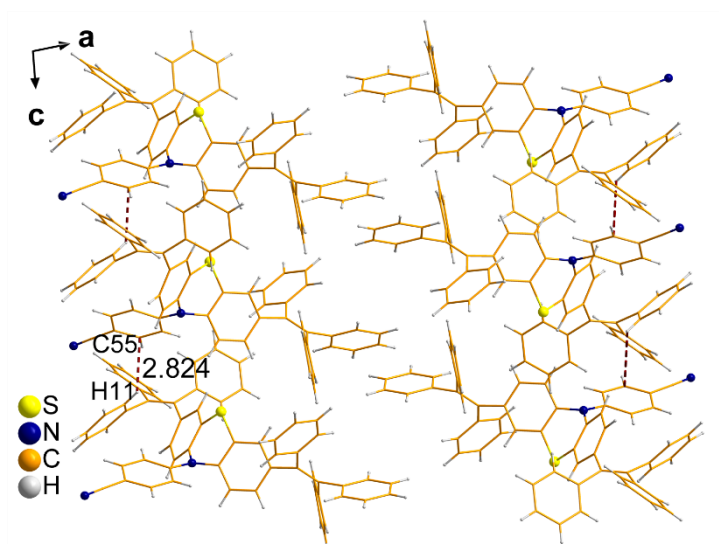


Fig. S5 Crystal packing diagram along the *b* axis.

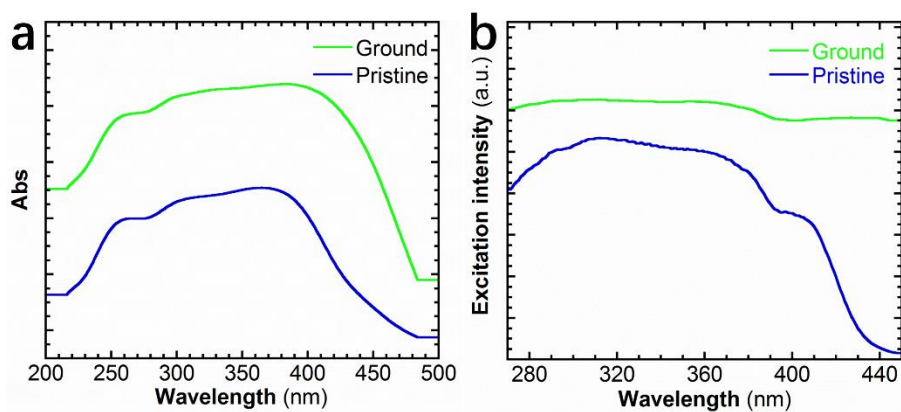


Fig. S6 (a) UV-vis absorption and (b) excitation spectra of solid powder of TPT before and after grinding.

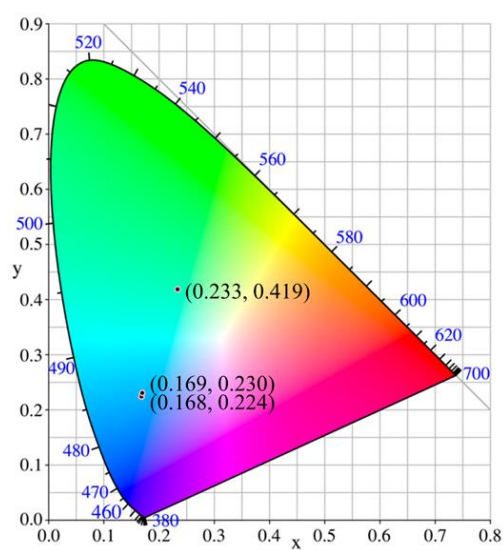


Fig. S7 CIE 1931 spectral chromaticity coordinates of TPT in different solid states.

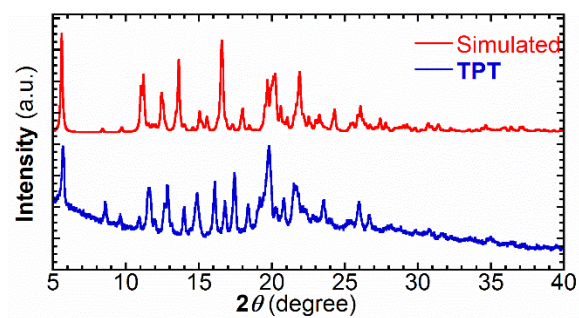


Fig. S8 powder X-ray diffraction and simulated patterns of **TPT**.

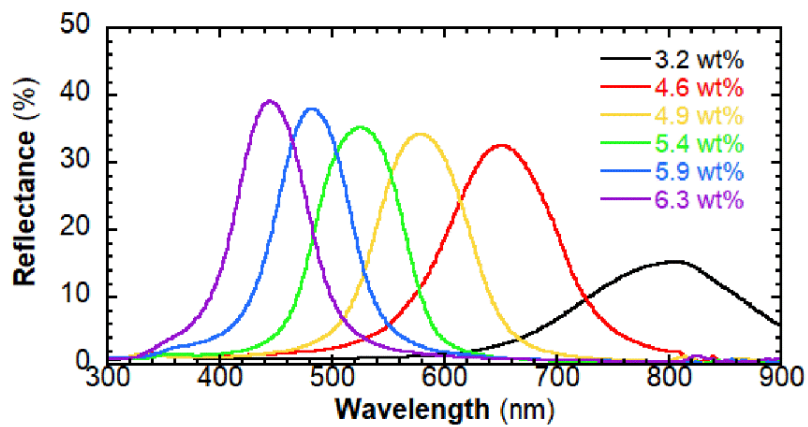


Fig. S9 UV-vis-NIR reflectance of CLC mixtures with different concentrations of CA taken before photopolymerization.

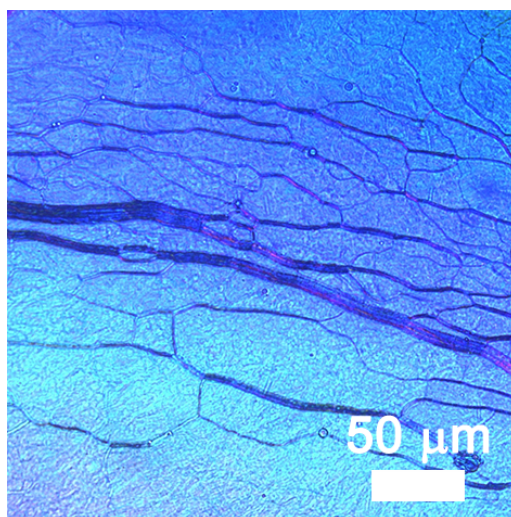


Fig. S10 POM image of LC242 with 1 wt% of **TPT** and 4.6 wt% of CA at 60 °C.

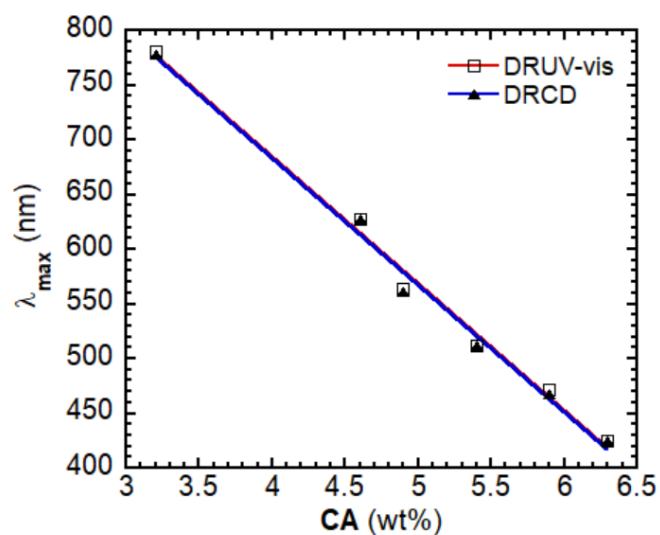


Fig. S11 Plots of λ_{\max} vs DRCD and DRUV-vis-NIR for **TPT-PSCLC** films.

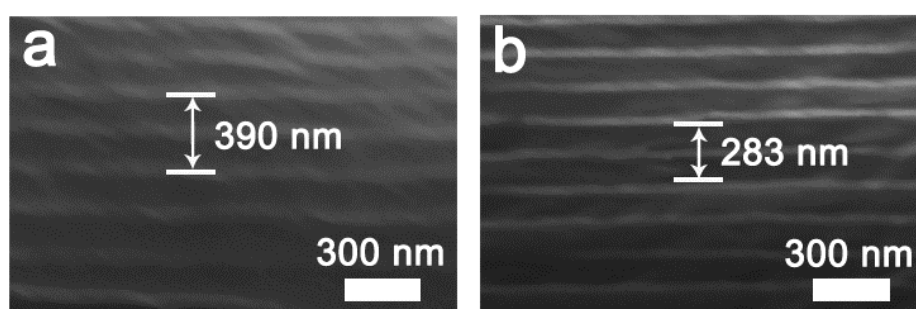


Fig. S12 Cross-sectional FE-SEM images the **TPT-PSCLC** films with (a) 4.6 and (b) 6.3 wt% of CA.

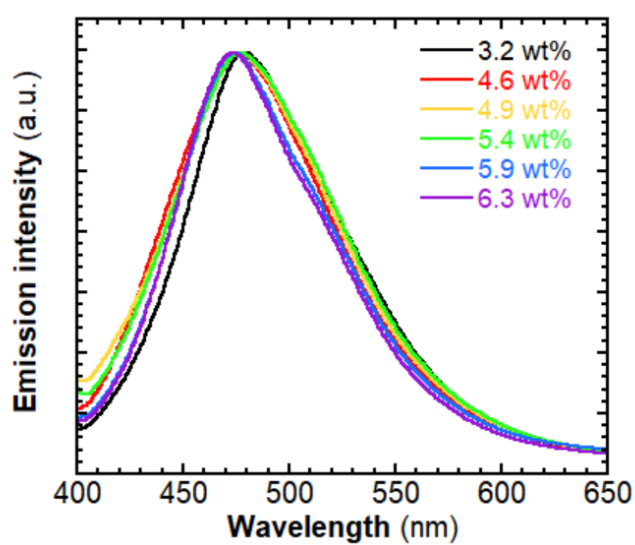


Fig. S13 Emission spectra of **TPT-PSCLC** films ($\lambda_{\text{ex}} = 340$ nm).

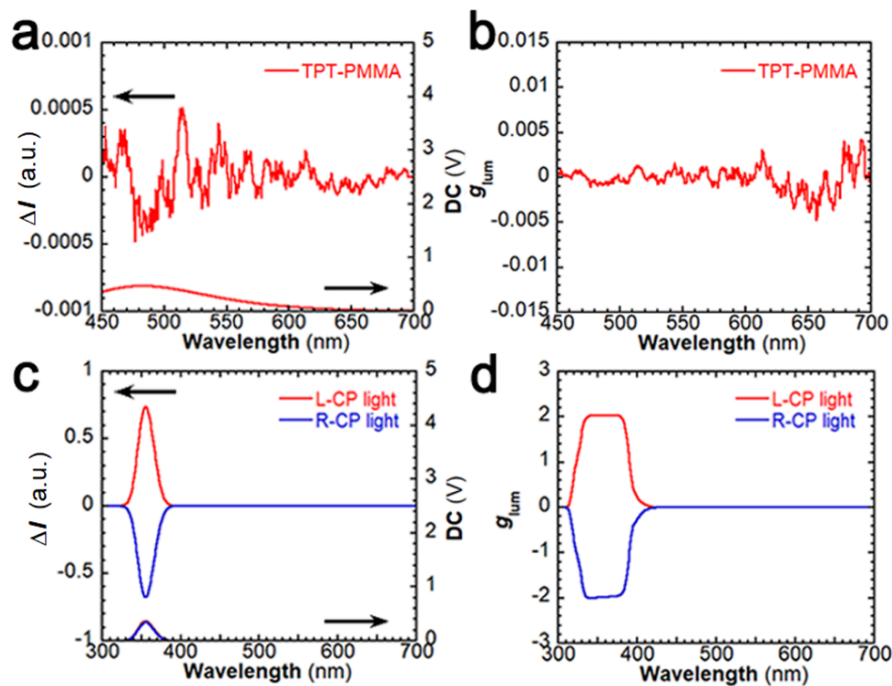


Fig. S14 (a) CPL spectra and (b) g_{lum} values of the TPT-PMMA film excited by nonpolarized light; (c) CPL spectra and (d) g_{lum} values of circularly polarized light with a wavelength of 355 nm.

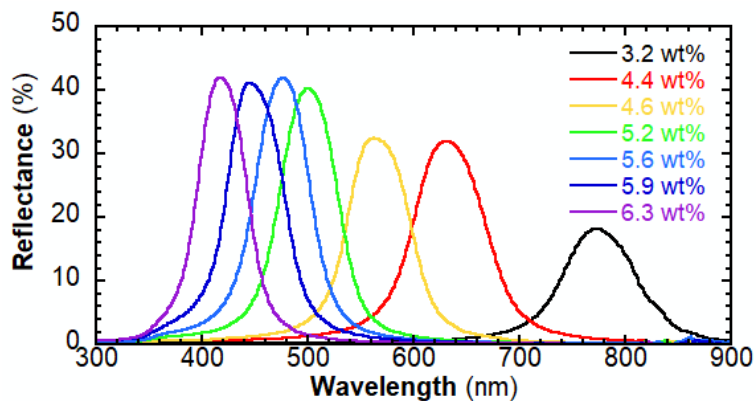


Fig. S15 UV-vis-NIR reflectance of PSCLC films without dye TPT.

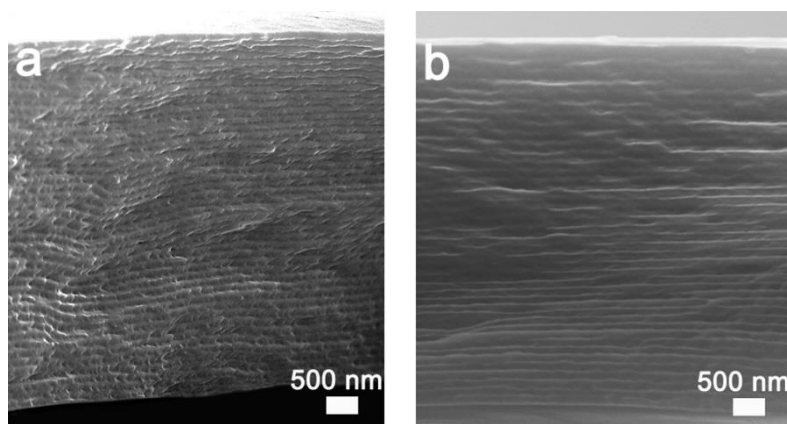


Fig. S16 Cross-sectional FE-SEM images of the PSCLC films with (a) 5.6 and (b) 6.3 wt% of CA.

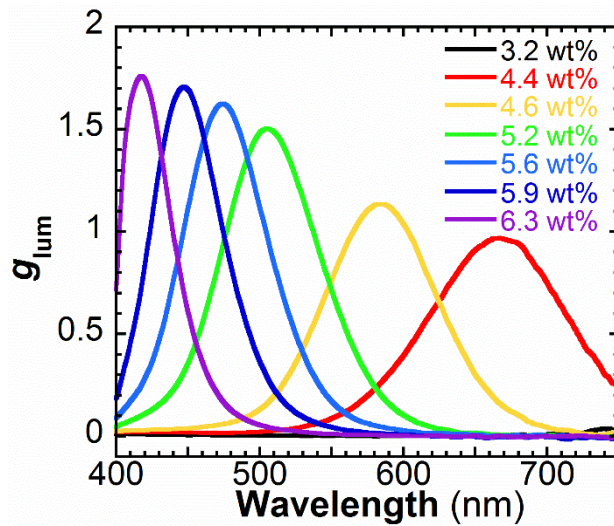


Fig. S17 g_{lum} values of TPT-PMMA film (1.0 wt% of dye) placed in front of a series of PSCLC films with different concentrations of CA excited by nonpolarized light ($\lambda_{ex} = 340$ nm).

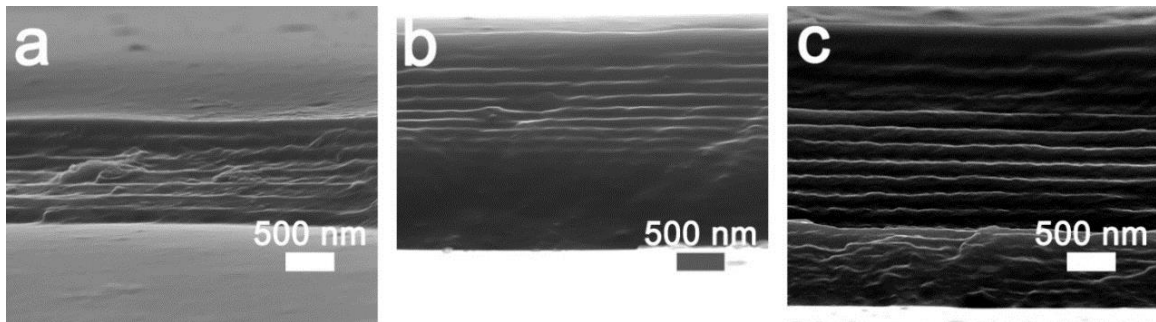


Fig. S18 Cross-sectional FE-SEM images of the PSCLC coated PET films with a thickness of (a) 1.0, (b) 2.2, and (c) 2.9 μm .

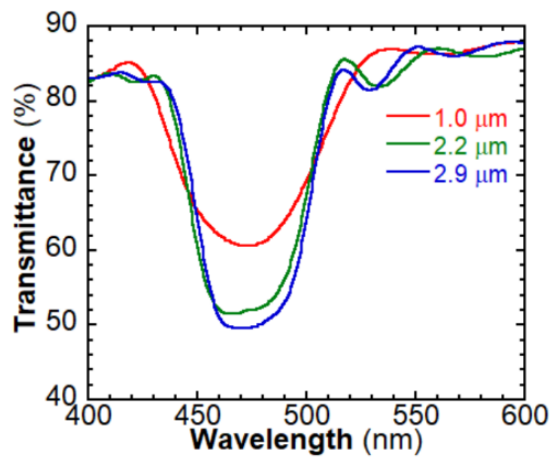


Fig. S19 Transmittance spectra of PSCLC coated PET films (1.0, 2.2, and 2.9 μm -thickness).

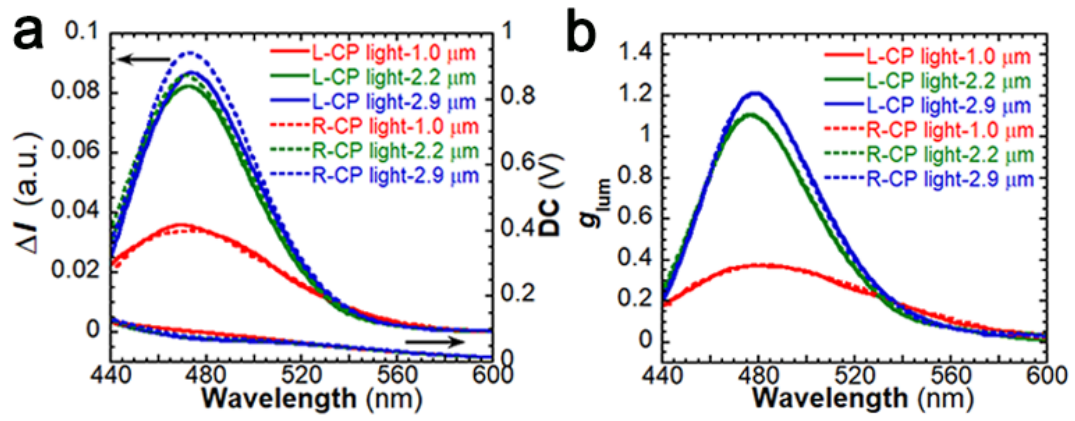


Fig. S20 (a) CPL spectra and (b) g_{lum} values of TPT-PMMA film (1.0 wt% of dye) located in front of PSCLC coated PET films with different thicknesses excited by circularly polarized light with a wavelength of 355 nm.